Article

Cationic, Neutral, and Anionic Allyl Magnesium Compounds: Unprecedented Ligand Conformations and Reactivity Towards Unsaturated Hydrocarbons

Crispin Lichtenberg, Thomas Paul Spaniol, Ilja Peckermann, Timothy P. Hanusa, and Jun Okuda

J. Am. Chem. Soc., **Just Accepted Manuscript** • DOI: 10.1021/ja310112e • Publication Date (Web): 14 Dec 2012

Revised

Cationic, Neutral, and Anionic Allyl Magnesium Compounds: Unprecedented Ligand Conformations and Reactivity Towards Unsaturated Hydrocarbons

Crispin Lichtenberg,[a] Thomas P. Spaniol,[a] Ilja Peckermann,[a] Timothy P. Hanusa,[b,] and Jun Okuda[a,]**

a: Institute of Inorganic Chemistry, RWTH Aachen University, Landoltweg 1, D-52056 Aachen, Germany

b: Department of Chemistry, Vanderbilt University, Nashville, Tennessee 37235, USA

RECEIVED DATE :

CORRESPONDING AUTHOR FOOTNOTE Institute of Inorganic Chemistry, RWTH Aachen University, Landoltweg 1, D-52056 Aachen, Germany. Fax: +49 241 80 92644. E-mail: jun.okuda@ac.rwth-aachen.de.

Department of Chemistry, Vanderbilt University, Nashville, Tennessee 37235, United States. E-mail: t.hanusa@vanderbilt.edu

Abstract

Starting from bis(allyl)magnesium [$Mg(C_3H_5)_2$], a set of cationic, neutral, anionic, and dianionic allyl magnesium compounds has been isolated and characterized, including $[Mg(C_3H_5)(THF)_5][B(C_6F_5)_4]$ (**3**), $[Mg(C_3H_5)_2(1,4\text{-dioxane})(THF)]$ (**2**), $[KMg(C_3H_5)_3(THF)]$

(**6**), and $[MMg(C_3H_5)_4]$ (**8**: M = K_2; **9**: M = Ca). In solution, the allyl ligands of the compounds display fluxional behavior, even at low temperatures. Single crystal X-ray analysis reveals unusual μ_2-η^1:η^3- and unprecedented μ_3-η^1:η^3:η^3 coordination modes in the heterobimetallic compounds **6** and [**8**·$(THF)_2$]. Density functional theory calculations confirm that these metal–allyl conformations are energetically stable. The magnesium compounds have been investigated as initiators for butadiene polymerization and ethylene oligomerization. The heterobimetallic compounds display initiation properties, including higher reaction rates, that are distinctively different from those of the monometallic species. Reactivity trends depend on the formal charge of the magnesium compounds (dianionic, higher order magnesiate > monoanionic, lower order magnesiate) and on the nature of the counterion ($K^+ > Ca^{2+}$).

Introduction

As the simplest delocalized carbanion, the allyl anion $(C_3H_5)^-$ is renowned for the flexibility it displays in its bonding and reactivity in metal complexes. Allyl magnesium complexes, for example, are commonly used as allyl transfer reagents in organic and organometallic chemistry.[1] Their characteristics in solution and in the solid state have been investigated in detail.[2] Further developments have led to heterobimetallic reagents that show reactivities distinct from their monometallic components. In particular, different selectivities and improved functional group tolerance in organic transformations as well as modified activities and selectivities in polymerization reactions have been reported.[3,4]

Such heterobimetallic magnesium species can be divided into two classes; firstly, “ate” compounds with magnesium counterions showing no Mg–allyl interactions; and secondly, magnesiates with the Mg–allyl bonds remaining intact. Significant differences in terms of structure and reactivity can be expected for these two types of compounds. Most heterobimetallic allyl magnesium species that have been investigated belong to the first

category, and heterobimetallic compounds containing $[Mg(C_3H_5)]^+$, $[Mg(C_3H_5)R_2]^-$ or $[Mg(C_3H_5)R_3]^{2-}$ fragments (R = allyl, alkyl) are rare. A few examples of *in situ* generated, ill-defined lithium allyl/alkyl magnesiates have been reported as allylation reagents in organic reactions.[3a-e] However, there are no detailed investigations dealing with the isolation, structure and reactivity of well defined heterobimetallic compounds containing Mg–allyl bonds. The development of reagents and catalysts based on earth-abundant, non-toxic metals is obviously an attractive goal, and toward this end we report the synthesis and characterization of a series of monocationic, neutral, monoanionic, and dianionic allyl magnesium compounds. These have been investigated both experimentally and computationally, and their reactivity towards butadiene and ethylene has been examined.

Results and Discussion

Neutral Allyl Magnesium Compound. Single crystals of a THF/dioxane adduct of $[Mg(C_3H_5)_2]$ (**1**) were analyzed for comparison with charged allyl magnesium species. $[Mg(\eta^1\text{-}C_3H_5)_2(THF)(\mu_2\text{-}1,4\text{-dioxane})]$ (**2**) crystallizes in the monoclinic space group *C*2/*c* with Z = 4 (Figure 1). The magnesium center is found in a trigonal bipyramidal coordination geometry with the η^1-bound allyl ligands and the THF ligand in the equatorial positions. The dioxane molecules occupy axial positions and their bridging coordination mode leads to a one-dimensional coordination polymer of **2** in the solid state. The coordination geometry around the magnesium center in **2** is closely related to those in the heterobimetallic complexes $[Ln(\eta^3\text{-}C_3H_5)_3(\mu_2\text{-}1,4\text{-dioxane})Mg(\eta^1\text{-}C_3H_5)_2(\mu_2\text{-}1,4\text{-dioxane})_{1.5}]$ (Ln = Y, La).[4e] However, in the latter compounds each magnesium center interacts with three bridging dioxane units, resulting in a two-dimensional network of dioxane-linked Mg_6Ln_4 macrocycles in the solid state. The Mg–C bond lengths in **2** are similar to those in the above mentioned heterobimetallic compounds. Mg–O(dioxane) bond lengths in **2** are ca. 0.18 Å longer than the

Mg–O(THF) bond length, which is due to the weaker donor character of the dioxane ligands and the fact that they occupy axial positions due to the *trans* influence.

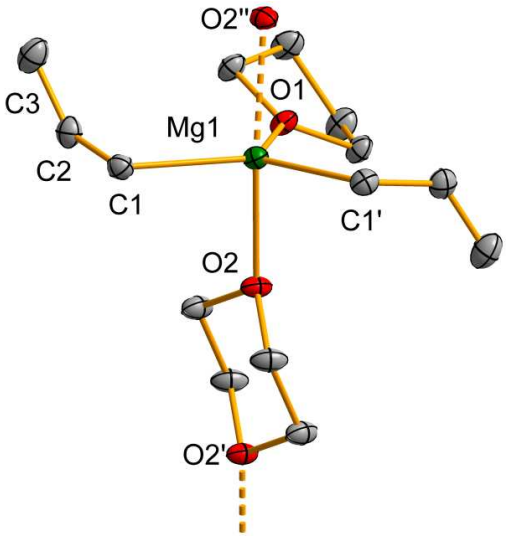

Figure 1. Molecular structure of $[Mg(\eta^1\text{-}C_3H_5)_2(THF)(\mu_2\text{-}1,4\text{-dioxane})]$ (**2**) in the solid state. Displacement ellipsoids are shown at the 50% probability level. Hydrogen atoms are omitted for clarity. Selected bond lengths [Å] and angles [°]: Mg1–C1, 2.2021(15); Mg1–O1, 2.0656(17); Mg1–O2, 2.2411(15); C1–C2, 1.4554(15); C2–C3, 1.3429(17); C1–Mg1–C1′, 126.66(7); C1–Mg1–O1, 116.67(4); C1–Mg1–O2, 92.33(4); O2–Mg1–O2′′, 163.59(5).

Cationic Allyl Magnesium Compound. Reaction of bis(allyl)magnesium (**1**) with one equivalent of the Brønsted acid $[NPhMe_2H][B(C_6F_5)_4]$ in THF allowed the isolation of the allylmagnesium monocation as a THF adduct, $[Mg(C_3H_5)(THF)_5][B(C_6F_5)_4]$ (**3**) (Scheme 1). It is noteworthy that perfluorination of the counterion was necessary, as the analogous reaction with the $[BPh_4]$ counterion led to THF-insoluble products. Colorless **3** is soluble in THF or dichloromethane, but insoluble in hydrocarbons and reacts with pyridine under carbometalation.[5,6] The allyl ligand in **3** shows fluxional behavior in dichloromethane at temperatures as low as –90 °C as revealed by ^{1}H NMR spectroscopy. Fluxional behavior of

allyl ligands at low temperature has also been reported for bis(allyl)magnesium,[7] whereas the η^1-bonding mode can be frozen out in the case of allyl Grignard reagents.[2c] Thus, the allyl exchange rate in allyl magnesium compounds is decreased by substitution of one allyl ligand for halides rather than by formation of a cation.

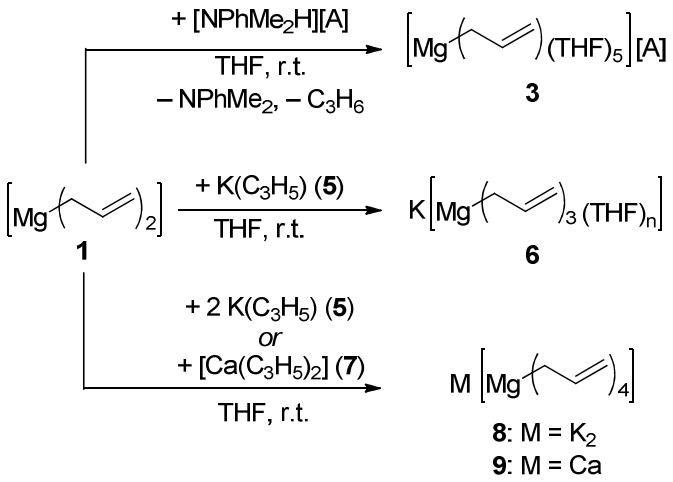

Scheme 1. Synthesis of charged allyl magnesium compounds: cationic **3**, lower order (monoanionic) magnesiate **6** as well as higher order (dianionic) magnesiates **8** and **9**; [A] = $[B(C_6F_5)_4]$; **6**: n = 0.5 or 1 (see main text and experimental).

The THF ligands in **3** give rise to one set of signals in the ^{1}H NMR spectrum in CD_2Cl_2 at ambient temperature. Upon cooling this sample to –90 °C, the THF resonances first broaden and finally split into two sets of signals of relative intensity 1:4. This is ascribed to an octahedral coordination geometry of the magnesium center in solution with the THF ligand *trans* to the allyl ligand being distinguishable from the four *cis*-THF ligands at low temperature (Scheme 2). For the exchange of THF ligands in *cis*- and *trans* positions, a rate constant of $k = 33\ s^{-1}$ was estimated at the coalescence temperature of $T_C = –20$ °C.

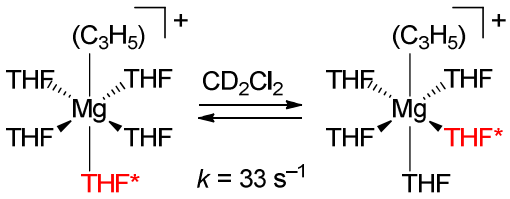

Scheme 2. Exchange of THF ligands in *cis*- and *trans* positions in compound **3**.

The THF ligands of **3** are labile in THF-d_8 solution and can be substituted for stronger donors as demonstrated by the formation of $[Mg(C_3H_5)(PMDTA)(THF)][B(C_6F_5)_4]$ (**4**) (PMDTA = *N*,*N*,*N*',*N*',*N*''-pentamethyldiethylenetriamine). **4** was analyzed by single crystal X-ray diffraction and crystallizes in the monoclinic space group $P2_1/c$ with $Z = 4$. The magnesium atom shows a coordination number of five and no interactions with the counterion are observed (Figure 2). The magnesium center is found in a distorted square pyramidal coordination geometry with the allyl ligand occupying the apical position.[8] The

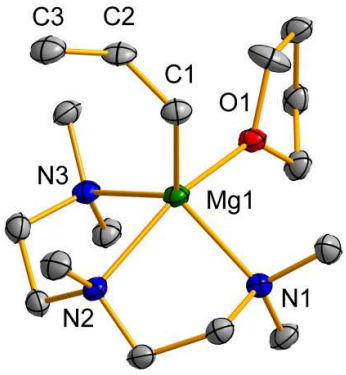

Figure 2. Cationic part of molecular structure of **4** in the solid state. Displacement ellipsoids are shown at the 50% probability level. Hydrogen atoms are omitted for clarity. Selected bond lengths [Å] and angles [°]: Mg1–C1, 2.181(3); Mg1–N1-3, 2.198(3)-2.295(3); Mg1–O1, 2.127(2); C1–C2, 1.447(5); C2–C3, 1.323(5); C1–Mg1–N1, 108.52(12); C1–Mg1–N2, 103.66(12); C1–Mg1–N3, 120.12(12); C1–Mg1–O1, 98.94(12); N1–Mg1–N2, 80.30(9); N1–Mg1–N3, 130.32(10); N1–Mg1–O1, 93.19(9); N2–Mg1–N3, 79.26(9); N2–Mg1–O1, 157.39(10); N3–Mg1–O1, 88.96(9); C1–C2–C3, 129.4(3).

allyl ligand adopts an η^1-bonding mode with the Mg–C(allyl) bond being slightly shortened compared to the corresponding value in neutral $[Mg(\eta^1\text{-}C_3H_5)_2(THF)(\mu_2\text{-}1,4\text{-dioxane})]$ (**2**) (2.181(3) Å vs. 2.2021(15) Å; *vide supra*). The preference of the allyl ligand for η^1-bonding at magnesium centers in the presence of donor ligands is well established for neutral compounds.[2f,g] Our results indicate that these findings can be extended to monocationic magnesium species. In comparison, polyhapto bonding has been reported for the related cyclopentadienyl compound $[Mg(\eta^5\text{-}C_5H_5)(PMDTA)][C_5H_5]$.[9]

Monoanionic Allyl Magnesium Compound. The potassium tris(allyl)magnesiate $[KMg(C_3H_5)_3(THF)_n]$ (**6**) was obtained by reaction of stoichiometric amounts of allyl potassium (**5**) with bis(allyl)magnesium (**1**) in THF (Scheme 1). **6** contains stoichiometric amounts of THF (n = 1) when crystallized and dried at ambient pressure, and substoichiometric amounts of THF (n = 0.5) when dried *in vacuo*. The magnesiate is soluble in THF, insoluble in diethyl ether or hydrocarbons and reacts under carbometalation with pyridine.[5,10] The allyl ligands in **6** show fluxional behavior in THF solution as revealed by an AX_4 pattern in the ^{1}H NMR spectrum, which only shows slight broadening of the signals at temperatures as low as –95 °C. Thus, no experimental indications could be obtained that **6** undergoes equilibrium reactions to reform the starting materials **1** and **4**.

Single crystals of **6** (n = 1) were obtained by gas phase diffusion of toluene into a solution of **6** in THF at ambient temperature. **6** crystallizes in the monoclinic space group $P2_1/m$ with Z = 2 (Figure 3). The atoms Mg1, K1, O1, and C1 are located within a crystallographic mirror plane. Mg1 is tetrahedrally coordinated by the THF ligand and by three η^1-bonded allyl ligands.[11] The potassium center K1 is coordinated by allyl ligands of four different $[Mg(C_3H_5)_3(THF)]^-$ units. The allyl ligands show η^3-, η^2-, and weak η^1-interactions[12] with K1 resulting in a distorted octahedral coordination geometry. This is the first example of one metal center interacting with six allyl ligands.

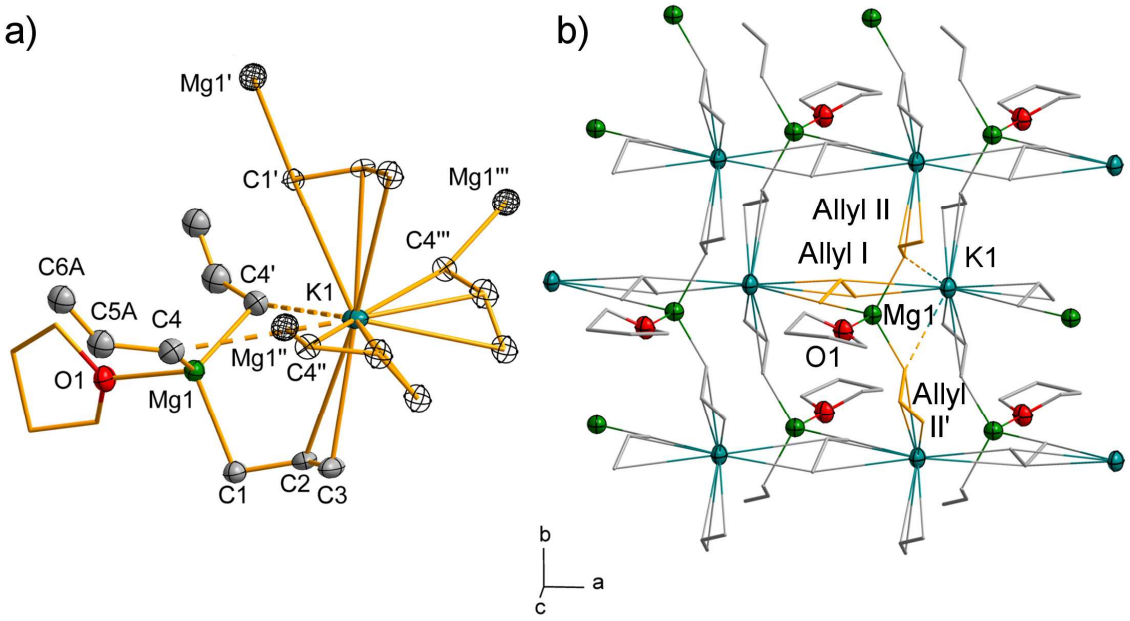

Figure 3. Molecular structure of **6** in the solid state. a) Coordination geometry around Mg and K. Displacement ellipsoids are shown at the 30% probability level. Hydrogen atoms are omitted for clarity; disordered carbon atoms are shown with one split position. Atoms that exceed one formula unit of **6** are drawn as empty ellipsoids. b) Two dimensional arrangement of **6** in the solid state. Carbon atoms are shown in wire frame model. Allyl I, II$^{(')}$ refers to C1-3, and C4$^{(')}$-6$^{(')}$, respectively. Selected bond lengths [Å] and angles [°]: Mg1–C1, 2.238(5); Mg1–C4, 2.212(4); Mg1–O1, 2.068(4); K1–C2, 3.575(6); K1–C3, 3.129(6); K1–C1', 3.103(5); K1–C2', 3.111(6); K1–C3', 3.466(6); K1–C4', 3.791(4); K1–C4'', 3.179(4); C4–Mg1–C4', 122.6(2); C4–Mg1–O1, 106.49(11).

Compound **6** displays two different kinds of allyl ligands in the solid state.[13] Firstly, two allyl ligands (Allyl II,II') interact with two different metal centers (with Mg (η^1) and with K (η^3)) resulting in a μ_2-η^1:η^3-coordination mode (Figure 3). Only few examples of complexes containing functionalized allyl ligands have been reported to adopt this coordination mode.[2e,f,14] **6** is the first example of the parent allyl ligand to show this structural feature.[15] Secondly, one allyl ligand in **6** (Allyl I) interacts with three metal centers (with Mg (η^1) and with K (η^2,η^3)) resulting in a μ_3-η^1:η^2:η^3-coordination mode (Figure 3). Such a coordination mode of the allyl ligand is unprecedented and adds a new facet to the coordination chemistry

of this small π-electron system. The average Mg1–C bond length of 2.23 Å (ranging from 2.212(4) to 2.238(5) Å) is much larger than the corresponding value of 1.996(8) Å in the only other fully characterized charged allyl magnesium species, $[Mg(C_3H_5)_4]^{2-}$.[16] This is ascribed to the simultaneous interaction of the allyl ligands in **6** with two or three metal centers, whereas the allyl ligands in the previously reported $[Mg(C_3H_5)_4]^{2-}$ dianion bind exclusively to one magnesium center. The effect of elongated metal carbon bonds due to interaction of one allyl ligand with multiple metal centers is also observed for the K–C distances in **6**, which range from 3.103(5) Å to 3.575(6) Å. The highest values exceed K–C distances found for η^3-allyl potassium compounds (2.87 Å - 3.15 Å),[17] but fall into the range of $K–C^{olefin}$ bonding (cut off value: K–C, 3.57 Å).[18] The C–C distances in the allyl ligands hint at predominant charge localization at the terminal carbon atom bound to Mg, which agrees with the literature.[2f,14,19] The bridging bonding modes of the allyl ligands lead to a two dimensional network of **6** in the solid state (Figure 3b). Potassium centers are connected via allyl ligands (Allyl I) to form an infinite chain along the *a*-axis. In perpendicular direction, the potassium and magnesium centers are linked by allyl ligands (Allyl II,II') to form infinite K/Allyl II/Mg/Allyl II' chains along the *b*-axis.

Dianionic Allyl Magnesium Compounds. Reaction of bis(allyl)magnesium with two equivalents of allyl potassium (**5**) or one equivalent of bis(allyl)calcium (**7**) in THF gave the dipotassium tetrakis(allyl)magnesiate $[K_2Mg(C_3H_5)_4]$ (**8**) and calcium tetrakis(allyl)magnesiate $[CaMg(C_3H_5)_4]$ (**9**), respectively (Scheme 1).[20] The allyl ligands in **8** and **9** show fluxional behavior at ambient temperature in THF as indicated by an AX_4 signal pattern in the ^1H NMR spectrum. The signals only broaden at temperatures as low as –95 °C. Thus, no experimental indication could be obtained that **8** or **9** undergo equilibrium reactions to reform monometallic starting materials **1**, **5** and **7**, respectively. In case of **9** a composition $Ca[Mg(C_3H_5)_4]$ is assumed, rather than the presence of an ion pair such as

$Ca(C_3H_5)][Mg(C_3H_5)_3]$, as the ^{1}H NMR resonances of the allylcalcium monocation clearly shows a different coupling pattern in THF-d_8.[21]

Single crystals of [**8**·$(THF)_2$] were obtained by cooling a saturated solution in THF/pentane to –30 °C. [**8**·$(THF)_2$] crystallizes in the monoclinic space group $P2_1/c$ with Z = 4 (Figure 4). The magnesium center interacts with four allyl ligands in an η^1-fashion resulting in a distorted tetrahedral coordination geometry (Figure 4a). No Mg–THF interactions are observed in the solid state, which is in contrast to the bonding situation found in monoanionic tris(allyl)magnesiate **6**. One of the crystallographically independent potassium atoms in [**8**·$(THF)_2$], K1, is coordinated by one THF ligand and by four allyl groups ($1 \times \eta^2$; $3 \times \eta^3$) resulting in a distorted trigonal bipyramidal coordination geometry with the η^2-allyl and the THF ligand in the axial positions. Three of the allyl ligands bind to K1 as donors of a chelating $[Mg(C_3H_5)_4]^{2-}$ group (Allyl I-III; Figure 4a). The fourth allyl group, Allyl IV, acts as a bridging ligand between K1 and a neighboring Mg1'. The second potassium center, K2, interacts with three allyl ligands ($3 \times \eta^3$) of three different neighboring $[Mg(C_3H_5)_4]^{2-}$ units and with one THF molecule, resulting in a distorted tetrahedral coordination geometry (Figure 4b). The allyl ligands in [**8**·$(THF)_2$] show two different types of coordination modes in the solid state, resembling the bonding situation found for **6** (*vide supra*). (i) Allyl IV interacts with two different metal centers resulting in a μ_2-η^1:η^3-coordination. (ii) Allyl I-III interact with three metal centers in a μ_3-η^1:η^2:η^3- or μ_3-η^1:η^3:η^3-fashion. The Mg–C distances in [**8**·$(THF)_2$] range from 2.175(18) to 2.41(4) Å and average 2.27 Å, which is clearly elongated compared those in the previously reported $[Mg(C_3H_5)_4]^{2-}$ ion.[16] K–C distances range from 2.932(13) Å to 3.481(7) Å. The highest values are larger than K–C distances found for η^3-allyl potassium compounds (2.87 Å - 3.15 Å),[17] but fall into the range of K–C^{olefin} bonding (cut off value: K–C, 3.57 Å).[18] As in case of compound **6**, the effect of elongated M–C distances was ascribed to each allyl ligand interacting with two or three metal centers. In agreement with the literature, the allyl ligands in [**8**·$(THF)_2$] show strongly localized C–C

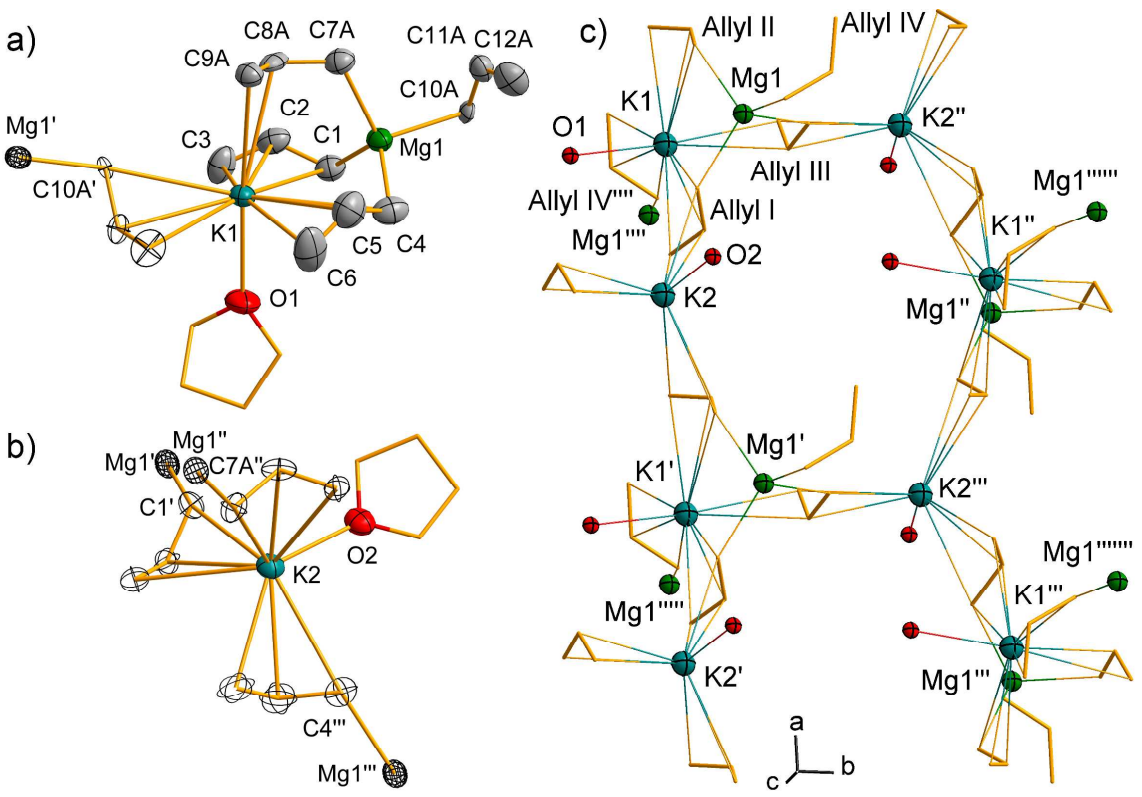

Figure 4. Cutouts of solid state structure of $[K_2Mg(C_3H_5)_4(THF)_2]$ ($[\mathbf{8}\cdot(THF)_2]$). Displacement ellipsoids are shown at the 50% probability level. Hydrogen atoms are omitted for clarity, disordered carbon atoms are shown with one split position Coordination geometries around Mg1 and K1 (a) and K2 (b). Atoms that exceed one formula unit of $[\mathbf{8}\cdot(THF)_2]$ are drawn as empty ellipsoids. c) Arrangement of $([\mathbf{8}\cdot(THF)_2]$ as a three dimensional coordination polymer with carbon atoms shown as wire frame (C^{allyl}) or omitted for clarity (C^{THF}). Allyl I-IV refers to C1-3, C4-6, C7-10, and C10-12, respectively. Selected bond lengths [Å] and angles [°]: Mg1–C1, 2.253(6); Mg1–C4, 2.254(6); Mg1–C7A, 2.29(2); Mg1–C7B, 2.26(3); Mg1–C10A, 2.175(18); Mg1–C10B, 2.41(4); K1–C1, 3.301(6); K1–C2, 3.144(6); K1–C3, 3.082(6); K1–C4, 3.481(7); K1–C5, 3.135(7); K1–C6, 3.044(7); K1–C7A, 3.87(3); K1–C8A, 3.155(8); K1–C9A, 3.22(7); K1–C10A, 3.242(18); K1–C11A, 3.056(9); K1–C12A, 3.18(2); K1–O1, 2.671(4); K2–C1, 3.165(6); K2–C2, 3.039(6); K2–C3, 3.243(6); K2–C4, 3.334(6); K2–C5, 3.049(8); K2–C6, 3.082(7); K2–C7A, 3.06(2); K2–C8A, 2.991(8); K2–C9A, 3.14(7); K2–O2, 2.709(4); C1–C2, 1.447(8); C2–C3, 1.311(9); C4–C5, 1.454(10); C5–C6, 1.306(11); C7A–C8A, 1.52(3); C8A–C9A, 1.37(6); C10A–C11A, 1.441(19); C11A–C12A, 1.37(2).

bonds (Δ_{C-C} = 0.07 Å to 0.15 Å).[2f,14] The bridging bonding modes of the allyl ligand result in a three dimensional network of [**8**·$(THF)_2$] in the solid state (Figure 4c).[22] Specifically, infinite chains of Allyl II/K1,Mg1/Allyl I/K2 along the *a*-axis, K1,Mg1/Allyl III/K2 along the *b*-axis, and K1/Allyl I-III/Mg1/Allyl IV along the *c*-axis are observed. Neighboring chains along the *a*-axis are related by a glide reflection along the *b*-axis. Only a few organometallic ate compounds of group 2 metals have been shown to form one[23] or two dimensional[24] carbanion-bridged coordination polymers in the solid state. While **6** adds to the examples of the latter category, the solid state structure of [**8**·$(THF)_2$] demonstrates that well defined three-dimensional networks can also be formed by this class of compounds. This is possible due to the unprecedented μ_3-η^1:$\eta^{2(3)}$:η^3-coordination mode of the allyl ligand found for [**8**·$(THF)_2$] (and for **6**), in which the $(C_3H_5)^-$ fragment acts as a T-shaped linker between three different metal centers.

Computational Results. The unusual metal–ligand bonding arrangements displayed by the allyls in the polymeric structures of **6** and **8** were investigated with a series of DFT calculations on various discrete model compounds. As the goal was to reproduce specific metal–allyl arrangements, rather than to duplicate exactly the coordination environments around the metals, in some cases methyl groups and additional THF ligands were used to complete the metal coordination spheres.

A. The Mg/K μ_2-η^1:η^3-allyl interaction. Attempts to model the μ_2-η^1:η^3 interaction (found in both **6** and **8**) with a MgR_2 (R = CH_3, C_3H_5, or H) fragment and K^+ placed on opposite sides of a $(C_3H_5)^-$ anion were unsuccessful. Regardless of the asymmetry of the starting conformation, geometry optimization consistently led to μ_2-η^3:η^3 structures with the Mg and K atoms centered or nearly centered over the allyl plane (see Supporting Information for an example). The results reflect the preference for Mg to engage in symmetrical η^3 bonding to allyls in the absence of sufficient perturbation (e.g., coordinated ethers).[2f] This

contrasts with the behavior of allyl zinc compounds which favor σ-type M–allyl interactions regardless of the presence of donor ligands.[25]

Addition of a single THF to the MgR_2 fragment causes a shift to a stable μ_2-η^1:η^3 interaction (**10a**, Figure 5a). The asymmetric position of the Mg relative to the allyl is evident in the Mg–C1 distance of 2.416 Å and the Mg···C2 separation of 2.900 Å; the corresponding

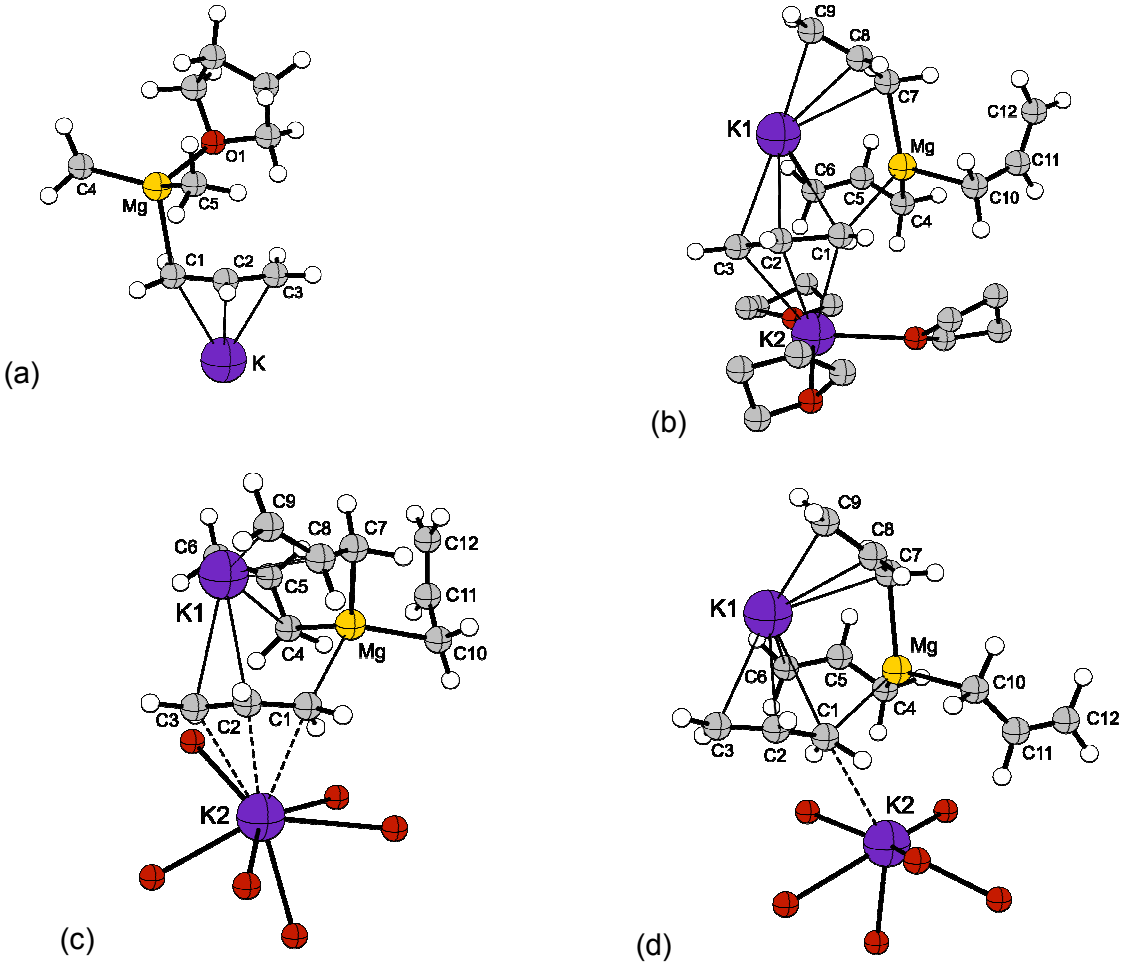

Figure 5. Calculated structures of Mg/K allyl complexes: (a) **10a** $[(CH_3)_2Mg(THF)(C_3H_5)K]$; (b) **10b** $[(C_3H_5)Mg(C_3H_5)_2K(C_3H_5)K(THF)_3]$ (hydrogen atoms have been omitted from the THF ligands for clarity); (c) **10c** and (d) **10d** $[(C_3H_5)Mg(C_3H_5)_2K(C_3H_5)][K(THF)_6]$ (only the oxygen atoms of the THF ligands are shown; dotted lines represent closest approaches of the potassium to the allyl ligands).

Mg–C1–C2 angle is 94.9°. The small difference between the C–C bonds in the allyl (C1–C2 = 1.412 Å; C2–C3 = 1.390 Å) suggests that the π electrons in the ligand are largely delocalized. The potassium is still nearly centered over the allyl plane (K–C1 = 2.810 Å; K–C3 = 2.788 Å).

Additional analysis supports the bonding picture suggested by the geometric parameters. The Nalewajski-Mrozek (N-M) bond index, which takes into account both covalent and ionic contributions to bonding,[26] is useful in this regard. The N-M indices between the Mg–C(methyl) bonds average 0.51; in contrast, the Mg–C1 and K–C1 bond indices are 0.10 and 0.17, respectively, indicating weak but not negligible interaction between the atoms (that between Mg and the oxygen in the THF, for example, is 0.12).

B. The Mg/K$_2$ μ_3-η^1:η^3:η^3-allyl interaction. As with the μ_2-η^1:η^3 interaction, attempts to model a trimetallic μ_3-η^1:η^3:η^3 arrangement using only the metals and allyl anions (i.e., with $[K(\eta^3\text{-}C_3H_5)K]^+$ and $[Mg(C_3H_5)_3]^-$ fragments) were not successful. With THF ligands added to one of the potassium centers, however, stable arrangements displaying allyl μ_3-η^1:η^3:η^3 interactions could be generated. With three THFs, structure **10b** (Figure 5b) is obtained. K2 is η^3–bonded to C1/C3 at distances in the narrow range from 3.085 Å to 3.090 Å. K1 is also η^3–bonded to C1/C3, but over a larger range (2.955 Å–3.197 Å); the bond distances in the allyl are consistent with substantial localization of the π-electrons (C1–C2 = 1.521 Å; C2–C3 = 1.388 Å). In addition, K1 is η^3–bonded to C7/C9 (2.986 Å–3.066 Å), and the π-electrons in C7/C9 are also localized (C7–C8 = 1.450 Å; C8–C9 = 1.364 Å). K1 displays a contact to C6 at 3.201 Å; contact distances to C4 and C5 are >3.5 Å, and can be considered to be nonbonding. The Mg–C1 contact is 2.626 Å, which is substantially longer than the bonds from Mg to C4, C7, and C10 (2.191–2.414). In total, the allyls in contact with Mg display four different bonding modes: μ_3-η^1:η^3:η^3, μ_2-η^1:η^3, μ_2-η^1:η^1, and simple η^1. In addition, the

experimentally observed trend that M–allyl bond lengths increase with the number of metal centers interacting with the allyl ligand was reproduced in the calculated model compounds.

The N-M bond indices generally support the bonding picture suggested by the geometric parameters. The Mg–C1 index is 0.16, roughly half the average of the Mg–C(4,7,10) values (0.31), but about the same as the average K2–O(THF) indices (0.13). There is no evidence, either in **10b** or in the structures below, for any substantial interaction between Mg and K1.

The addition of more THF molecules to K2 provides some simulation of the effect of solvation, and a measure of the robustness of the metal–allyl interactions. With three more THF ligands on K2, the resulting structure minimizes to that of **10c** (Figure 5c). Although complete separation of charged fragments will not occur under the (gas-phase) conditions of the calculations, analysis of the interactions suggests that appreciable fractionation into $[KMg(C_3H_5)_4]^-$ and $[K(THF)_6]^+$ units has occurred. One metric for this is the distance from K1 to K2, which is 5.21 Å in **10b**, but 5.68 Å in **10c**. In addition, the average K2–C distance has increased from 3.088 Å in **10b** to 3.159 Å in **10c**. Based on distance criteria, the interaction of K1 with the C1/C3 allyl is now η^2; i.e., K1–C3 = 3.082 Å, K1–C2 = 3.091 Å, but K1···C1 = 3.554 Å.[27] The bonding of K1 to the C7/C9 allyl is η^3 (distances range from 3.009-3.115 Å); the same is true for the C4/C6 allyl (distances range from 3.023-3.056 Å). The Mg–C1 distance is 2.376 Å, a shrinkage of 0.25 Å from the value in **10b**. The N-M bond index for Mg–C1 has slightly increased to 0.19, and is now appreciably larger than the average K2–O(THF) indices (0.08), which have collectively weakened compared to the value in **10b** (this mirrors the longer average K–O bond length in **10c** (3.04 Å) compared to **10b** (2.72 Å).

Owing to the highly polarized bonding associated with the K^+ and Mg^{2+} cations, ligand rearrangements need not require much energy in these systems. For example, with a slightly different arrangement of the THF ligands (obtained by successively adding THFs to **10b**, and reminimizing the energy after each addition), structure **10d** (Figure 5d) is obtained. The

immediately obvious difference from **10c** is that K2 is η^1-bonded to C1/C3; the distance to C1 is 3.211 Å, but that to C2 and C3 is >4.3 Å. K1 remains η^3-bonded to C1/C3, although in a slightly distorted fashion (2.959-3.180 Å); it is also η^3–bonded to C7/C9 over a narrower range (2.954-3.055 Å). The Mg–C1 distance is now 2.405 Å. The N-M bond indices support these structural assignments; the K2–C1 index is 0.03, consistent with very weak η^1-bonding between the metal and allyl, and the interaction of Mg–C1 has a bond index of 0.21, compared to an average of 0.29 for the bonds from Mg to C4, C7, and C10.

The sensitivity of the allyl alignments to the number of THFs on the potassium reflects the relatively flat potential energy surface associated with the Mg^{2+} and K^+ centers. Despite what appears to be substantial differences in the bonding arrangements of **10c** and **10d**, particularly as regards the relationship of K2 to the C1/C3 allyl, both represent local minima on their potential energy surfaces (N_{imag} = 0), and the two structures differ by only 2.5 kcal mol^{-1} in $\Delta H°$ (1.1 $kcal^{-1}$ mole in $\Delta G°$; **10d** is the lower). The small energy difference between the two structures underscores the weak association of the $[KMg(C_3H_5)_4]^-$ and (highly distorted) $[K(THF)_6]^+$ fragments.

Butadiene Polymerization. Heterobimetallic allyl ate compounds of rare earth elements containing magnesium as the counterion have been investigated in detail as initiators for isoprene (co)polymerization.[4a,c,f,g] In contrast, similar investigations of magnesium based initiators containing Mg–C bonds are rare. Hsieh and coworkers reported on lithium (alkyl)magnesiate species as initiators for butadiene polymerization, which exhibit properties in these reactions that differ from those of their monometallic components.[28] However, the focus of that work was dedicated to the polymerization studies. The ate compounds were generated *in situ* by reaction of $[Mg(n\text{Bu})_2]$ with [Li(*n*Bu)], have not been characterized, and remain ill-defined. The K–allyl interactions found in the solid state structures of **6** and $[\mathbf{8}\cdot(THF)_2]$ encouraged us to compare the reactivity of cationic **3** and **4**, lower order (monoanionic) magnesiate **6**, and higher order (dianionic) magnesiates **8** and **9** towards the

simple delocalized π-electron system butadiene (BD). Cationic **3** and **4** showed no reaction with BD in coordinating or weakly coordinating solvents (Table 1, entry 1).[29] Monoanionic **6** polymerized BD in THF solution at 0 °C in a rapid, exothermic reaction to give polybutadiene (PBD) with a low polydispersity index (PDI) of 1.04 and a high 1,2-PBD content of 69% (entry 2). When dianionic potassium magnesiate **8** was used as an initiator, PBD with similar properties was obtained at a higher rate (entry 3).[30] BD polymerization initiated by the dianionic calcium magnesiate **9** gave PBD of higher 1,2-PBD content, lower molecular weight, and a slightly increased PDI at higher temperature and prolonged reaction times (entry 4). The living polymerization reactions initiated by **6**, **8**, and **9** show first order kinetics revealing reaction rates of k(**8**, –25 °C)[31] = 1.6 s^{-1}, k(**6**, 0 °C) = 6.9×10^{-1} s^{-1}, k(**9**, 45 °C) = 8.7×10^{-5} s^{-1} (for details see Supporting Information). Differences in the reactivity of higher order magnesiates **8** and **9** might be due to differences in the strength and polarity of the M–C interactions (M = K, Ca). Furthermore, equilibria between the higher order magnesiates and their corresponding lower order magnesiates and neutral compounds might play a role.[32] Altogether these results reveal that (i) in contrast to cationic allyl magnesium compounds, anionic allyl magnesium species initiate BD polymerization, (ii) the rate of reaction is higher for dianionic than for monoanionic potassium magnesiates,[33] and (iii) the counter ion (K^+ vs. Ca^{2+}) is crucial for determining reaction rates and to a lesser extent the selectivities of BD polymerization initiated by dianionic magnesiates. The BD polymerization initiators **6**, **8**, and **9** may be compared to literature known catalyst systems for this reaction. The production of PBD with high contents of *trans*-1,4-PBD (94%),[34] *cis*-1,4-PBD (>99.9%),[35,36] atactic 1,2-PBD (100%),[37] syndiotactic 1,2-PBD (99.7% 1,2-PBD; 99.6% syndiotacticity),[38] and isotactic 1,2-PBD (97-99% 1,2-PBD; 99% isotacticity)[39] has been reported. The microstructure of the PBD obtained from reactions initiated by **6**, **8**, and **9** (69-77% 1,2-PBD) is similar to that of PBD produced with alkyllithium initiators in polar media such as THF.[40,41,42] For further comparison, the monometallic components of heterobimetallic compounds **6**, **8**, and **9** were

also tested as initiators for BD polymerization. As expected, $[Mg(C_3H_5)_2]$ (**1**) did not react with butadiene under given conditions (entry 5). $[K(C_3H_5)]$ (**5**) did not initiate BD polymerization under standard conditions (entry 6),[43] but PBD with a slightly increased PDI was obtained upon increasing the catalyst loading (entry 7), revealing the high sensitivity of **5** towards trace impurities in the monomer solution. In turn, this demonstrates the increased robustness of compounds **6** and **8**. $[Ca(C_3H_5)_2]$ (**7**) has been reported to act as an initiator for BD polymerization (entry 8).[44] In comparison, heterobimetallic **9** gave PBD with a lower PDI value and a higher 1,2-PBD content at a significantly higher rate. In summary, properties distinct from their monometallic components have been revealed for heterobimetallic compounds **6** and **8** (higher robustness, lower PDI) as well as **9** (higher reaction rate, higher 1,2-PBD content, lower PDI) when applied as initiators for BD polymerization.

Table 1. Butadiene polymerization with initiators **1** and **3**-**9**.

Entry	Initiator	[BD] / [Initiator]	*T* [°C]	*t* [min]	Yield [%]	Microstructure of PBD [%]			M_n [g/mol]	M_w/M_n
						1,2-	*cis*-1,4-	*trans*-1,4-		
1[a]	$[Mg(C_3H_5)(THF)_5][A]$ (**3**)	200	45	1200	0	-	-	-	-	-
2	$[KMg(C_3H_5)_3(THF)_{0.5}]$ (**6**)	200	0	4	>99	69	17	14	17300	1.04
3	$[K_2Mg(C_3H_5)_4]$ (**8**)	200	0	1	97	71	18	11	24600	1.04
4	$[CaMg(C_3H_5)_4]$ (**9**)	200	45	540	>99	77	14	9	7800	1.10
5	$[Mg(C_3H_5)_2]$ (**1**)	200	45	1200	0	-	-	-	-	-
6	$[K(C_3H_5)]$ (**5**)	200	0	4	0	-	-	-	-	-
7	$[K(C_3H_5)]$ (**5**)	50	0	4	>99	67	12	21	9200	1.17
8[44]	$[Ca(C_3H_5)_2]$ (**7**)	200	45	1200	75	47	17	36	39700	1.21

BD = butadiene; PBD = polybutadiene; [A] = $[B(C_6F_5)_4]$; reactions carried out in THF;
a: no reaction of **3** or **4** with BD was observed in reaction times of $t > 1$ d at temperatures of up to 50 °C (sealed tube), when CD_2Cl_2 was used as a solvent.

Reactivity Towards Ethylene. Reactivity studies of potassium, magnesium, and calcium compounds towards ethylene are rare. Cumylpotassium has been investigated as an initiator for the copolymerization of α-methylstyrene and ethylene at ambient temperature giving an

oligormer (M_n = 605 g/mol) with a low ethylene content of 15% corresponding to ca. one ethylene unit per oligomer in a slow reaction (t = 12 d).[45] Under more forcing conditions (60 °C, 40 bar C_2H_4), organoalkali compounds catalyze the oligoethylation of aromatic hydrocarbons.[46] While organomagnesium species alone have been reported to react with ethylene under high pressures at elevated temperature,[47] aryl Grignard reagents carbometalate ethylene in the presence of transition metal salts under less forcing conditions.[5,48] In this context, the allyl compounds that initiated the polymerization of BD were also tested in their reactivity towards ethylene. The calcium compound $[Ca(C_3H_5)_2]$ (**7**) was reported not to react with ethylene.[49] $[CaMg(C_3H_5)_4]$ (**9**) did not react with ethylene either (THF, r.t., 2 bar ethylene).[50] Under identical conditions, the more reactive potassium compounds $[K(C_3H_5)]$ (**5**), $[KMg(C_3H_5)_3(THF)_{0.5}]$ (**6**), and $[K_2Mg(C_3H_5)_4]$ (**8**) reacted with ethylene under carbometalation (Figure 6, for extended time conversion plots see Supporting Information).[5] This reaction was extremely slow, but selective for lower order magnesiate **6** (insertion of 2 equiv. of ethylene after t = 25 d, no side products detected by ^{1}H NMR spectroscopy, for details see Supporting Information). Organopotassium compound **5** expectedly showed an increased reactivity, but formation of side products was observed at early stages of the reaction (after consumption of 0.2 equiv. of ethylene). GC/MS analysis of the reaction

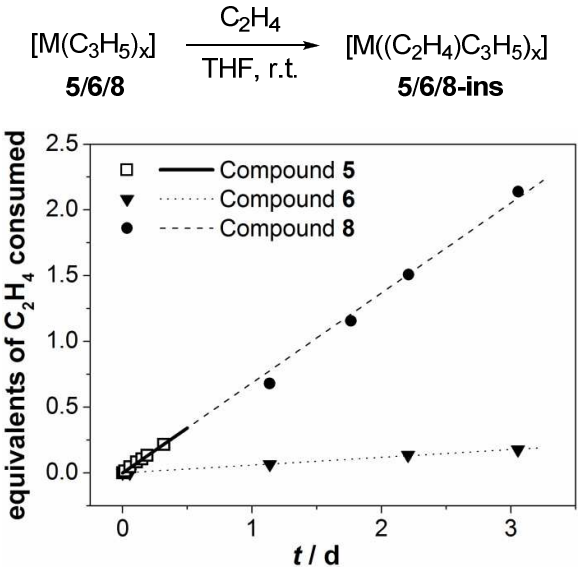

Figure 6. Course of reaction of compounds **5**, **6**, and **8** with ethylene.[5]

mixture after aqueous workup revealed a mixture of $C_{5\text{-}11}$-hydrocarbons resulting from multiple insertion of ethylene as the main components (for details see Supporting Information). For higher order magnesiate **8**, the rate of ethylene consumption is similar to that of **5**. However, selective monoinsertion is observed up to consumption of ca. 2 equiv. of ethylene, which was ascribed to the stabilizing effect of the magnesiate component. After prolonged reaction times, the reaction mixture was quenched with water and analyzed by GC/MS revealing a mixture of $C_{5\text{-}11}$ hydrocarbons similar to that observed in case of **5** (for details see Supporting Information). Thus, allyl potassium (**5**) and higher order magnesiate **8** insert ethylene more readily than cumyl potassium[45] and under milder conditions than neutral magnesium compounds such as [Mg(*n*Bu)$_2$] or [Mg(*n*Bu)Br],[47] but are significantly less active than any transition metal based catalysts.[51]

Conclusion

In order to clarify the structure and reactivity of heterometallic allyl complexes containing magnesium, a series of cationic, neutral, anionic and dianionic compounds has been isolated and characterized. Potassium or calcium centers balance the charge in case of the magnesiate complexes. In solution, the allyl ligands of all magnesium compounds show fluxional behavior, even at temperatures ≤ –90 °C.[7] In the solid state, the allyl magnesium compounds evidence the structural diversity of the allyl ligand as typical molecular structures (η^1-coordination; cationic and neutral compounds) and coordination polymers (μ_2-η^1:η^3- and μ_3-η^1:η^3:η^3-coordination; lower order (monoanionic) and higher order (dianionic) magnesiates) are observed. A description of the bonding situation in the unusual μ_2-η^1:η^3- and the unprecedented μ_3-η^1:η^3:η^3 coordination mode has been derived from structural parameters obtained by single crystal X-ray crystallography in combination with DFT calculations on

model compounds. The latter confirm that the metal–allyl interactions can be replicated in discrete molecules, and are not simply artifacts of the extended structures observed in the solid state. All magnesium compounds have been investigated as initiators for butadiene polymerization. Cationic $[Mg(C_3H_5)(THF)_5][B(C_6F_5)_4]$ and neutral $[Mg(C_3H_5)_2]$ do not initiate the polymerization of butadiene under the chosen conditions, but the heterobimetallic compounds $[KMg(C_3H_5)_3(THF)_n]$ (**6**, n = 0.5, 1), $[K_2Mg(C_3H_5)_4]$ (**8**), and $[CaMg(C_3H_5)_4]$ (**9**) give polybutadiene (PBD) with low polydispersity indices below 1.10 and high 1,2-PDB contents up to 77%. These compounds show initiation properties that are distinct from their monometallic components, such as increased robustness and higher reaction rates. The counterions, K^+ vs. Ca^{2+}, and the formal charge of the magnesiate have a strong effect on the reaction rates (K^+ > Ca^{2+}; higher order > lower order magnesiate). Whereas the calcium magnesiate **9** does not react with ethylene, $[K(C_3H_5)]$ (**5**) and the potassium magnesiates **6** and **8** react under insertion of 1 ethylene unit in case of **6** and 1-4 ethylene units per allyl ligand in case of **5** and **8**. Taken together, these results should broaden our understanding of the metal-ligand relationships that emerge from the interaction of multiple dissimilar metals and the allyl anion. This knowledge should help the design of new active catalyst incorporating the earth-abundant s-block metals.

Experimental

General Remarks. All operations were carried out under argon using standard Schlenk-line and glovebox techniques. Starting materials were purchased from Sigma Aldrich or Boulder Scientific and purified following standard laboratory procedures. $[Mg(C_3H_5)_2]$ (**1**), $[Ca(C_3H_5)_2]$ (**7**), and $[K_2Mg(C_3H_5)_4]$ (**8**) were prepared according to the literature.[2c,20,44a] Non-deuterated solvents were purified using an MB SPS-800 solvent purification system. THF-d_8 was distilled from sodium benzophenone ketyl. CD_2Cl_2 and pyridine-d_5 were distilled from

CaH_2. All NMR spectra were recorded at ambient temperature (if not stated otherwise) using a Bruker Avance II 400 MHz spectrometer. The chemical shifts of ^1H and ^{13}C NMR spectra were referenced internally using the residual solvent resonances and are reported relative to the chemical shift of tetramethylsilane. The resonances in ^1H and ^{13}C NMR spectra were assigned on the basis of two dimensional NMR experiments (COSY, HMQC, HMBC). The ^{11}B NMR resonances are reported relative to an external standard (an ethereal solution of $[BF_3{\cdot}Et_2O]$). Metal titrations were performed according to the literature. Molecular weights and polydispersities were determined by size exclusion chromatography in THF at ambient temperature, at a flow rate of 1 mL/min utilizing an Agilent 1100 Series HPLC, G1310A isocratic pump, an Agilent 1100 Series refractive index detector (at 35 °C) and 8 × 600 mm, 8 × 300 mm, 8 × 50 mm PSS SDV linear M columns. Calibration standards were commercially available narrowly distributed linear polystyrene samples that cover a broad range of molar masses ($10^3 < M_n < 2{\times}10^6$ g/mol). Microstructure determinations were performed according to the literature.[52]

$[Mg(\eta^1\text{-}C_3H_5)_2(THF)(\mu_2\text{-}1,4\text{-dioxane})]$ (2). Single crystals of **2** were obtained from a concentrated solution of $[Mg(C_3H_5)_2]$ (**1**) in THF/dioxane at –30 °C. Anal. calcd. for $C_{14}H_{26}MgO_3$ (266.66 g/mol): C, 63.06; H, 9.83; found: C, 62.31; H, 9.78.

$[Mg(\eta^1\text{-}C_3H_5)(THF)_5][B(C_6F_5)_4]$ (3). A solution of $[NPhMe_2H][B(C_6F_5)_4]$ (350 mg, 0.44 mmol) in THF (1.0 mL) was added to a solution of $[Mg(C_3H_5)_2]$ (47 mg, 0.44 mmol) in THF (0.5 mL). The reaction mixture was filtered. The filtrate was concentrated under reduced pressure to a volume of 1.0 mL. Upon addition of pentane (10 mL), a colorless solid precipitated, which was filtered off, washed with pentane (3 × 2.0 mL) and dried in vacuo. Yield: 449 mg, 0.41 mmol, 93%.

^1H NMR (400.1 MHz, THF-d_8): δ = 1.75-1.80 (m, 20H, β-THF), 2.43 (d, $^3J_{HH}$ = 11.4 Hz, 4H, CH_2CHCH_2), 3.60-3.64 (m, 20H, α-THF), 6.28 (quint, $^3J_{HH}$ = 11.4 Hz, 1H, CH_2CHCH_2) ppm. ^1H NMR (400.1 MHz, CD_2Cl_2, 23 °C): δ = 2.02-2.05 (m, 20H, β-THF), 2.56 (d, $^3J_{HH}$ = 11.3

Hz, 4H, CH_2CHCH_2), 3.89-3.92 (m, 20H, α-THF), 6.28 (quint, $^3J_{HH}$ = 11.3 Hz, 1H, CH_2CHCH_2) ppm. ^{1}H NMR (400.1 MHz, CD_2Cl_2, –60 °C): δ = 1.95-1.98 (m, 16H, β-THF^{eq}), 1.98-2.02 (m, 4H, β-THF^{ax}), 2.39 (d, $^3J_{HH}$ = 11.5 Hz, 4H, CH_2CHCH_2), 3.78-3.80 (m, 4H, α-THF^{ax}), 3.80-3.83 (m, 16H, α-THF^{ax}), 6.26 (quint, $^3J_{HH}$ = 11.5 Hz, 1H, CH_2CHCH_2) ppm. ^{13}C NMR (100.6 MHz, THF-d_8): δ = 26.38 (s, β-THF), 58.22 (s, CH_2CHCH_2), 68.36 (s, α-THF), 125.27 (br s, *ipso*-C_6F_5), 137.19 (dm, $^1J_{CF}$ = 247.1 Hz, *m*-C_6F_5), 139.19 (dm, $^1J_{CF}$ = 244.5 Hz, *p*-C_6F_5), 149.22 (dm, $^1J_{CF}$ = 241.0 Hz, *o*-C_6F_5), 149.50 (s, CH_2CHCH_2) ppm. ^{11}B NMR (128.4 MHz, THF-d_8): δ = –18.46 (s) ppm. Anal. calcd. for $C_{39}H_{29}BF_{20}MgO_3$ (1104.94 g/mol): Mg, 2.20; found: Mg, 2.51.

[Mg(η^1-C_3H_5)(PMDTA)(THF)][B(C_6F_5)$_4$] (4). A solution of PMDTA (8 mg, 0.046 mmol) in THF (0.5 mL) was added to a solution of **3** (50 mg, 0.045 mmol) in THF (0.5 mL). All volatiles were removed from the reaction mixture under reduced pressure. The residue was washed with pentane (3 × 1.5 mL), to give a colorless solid that was dried in vacuo. Yield: 45 mg, 0.045 mmol, quantitative.

^{1}H NMR (400.1 MHz, THF-d_8): δ = 1.76-1.80 (m, 4H, β-THF), 2.45 (s, 12H, NMe_2) 2.49 (d, $^3J_{HH}$ = 11.5 Hz, 4H, CH_2CHCH_2), 2.50-2.53 (m, 2H, (CH^aH^{b}CH^{c}H^d)), 2.53 (s, 3H, NMe), 2.65-2.68 (m, 2H, (CH^{a}H^{b}CH^cH^d)), 2.81-2.94 (m, 4H, (CH^aH^bCH^cH^d)), 3.60-3.64 (m, 4H, α-THF), 6.31 (quint, $^3J_{HH}$ = 11.5 Hz, 1H, CH_2CHCH_2) ppm. ^{13}C NMR (100.6 MHz, THF-d_8): δ = 26.53 (s, β-THF), 45.11 (s, NMe), 45.81 (br s, CH_2CHCH_2), 46.75 (br s, NMe_2), 55.95 (s, (CH^{a}H^bCH^{c}H^d)), 58.48 (s, (CH^aH^{b}CH^{c}H^d)), 68.39 (s, α-THF), 125.33 (br s, *ipso*-C_6F_5), 137.28 (dm, $^1J_{CF}$ = 246.2 Hz, *m*-C_6F_5), 139.29 (dm, $^1J_{CF}$ = 244.5 Hz, *p*-C_6F_5), 149.32 (dm, $^1J_{CF}$ = 245.4 Hz, *o*-C_6F_5), 149.41 (s, CH_2CHCH_2) ppm. ^{11}B NMR (128.4 MHz, THF-d_8): δ = –16.60 (s) ppm. Anal. calcd. for $C_{40}H_{36}BF_{20}MgN_3O$ (989.82 g/mol): Mg, 2.46; found: Mg, 2.36.

[K$Mg(C_3H_5)_3(THF)_n$] (n = 0.5, 1) (6). Method A (n = 0.5): K(C_3H_5) (75 mg, 0.94 mmol) was added to a solution of [$Mg(C_3H_5)$]$_2$ (**1**) (100 mg, 0.94 mmol) in THF (2.0 mL). The

reaction mixture was filtered. Upon addition of pentane (3.0 mL) to the filtrate, a colorless solid precipitated, which was isolated by decantation, washed with pentane (3 × 2.0 mL) and dried in vacuo. Yield: 206 mg, 0.93 mmol, 99%.

Method B (n = 1): $[K(THF)_{0.5}][Mg(C_3H_5)_3]$ (50 mg) was dissolved in THF (0.5 mL). Pentane was added via gas phase diffusion at ambient temperature. After 3 d, colorless single crystals were obtained, which were isolated by decantation and dried at ambient pressure under inert gas atmosphere. Yield: 32 mg, 0.12 mmol, 55%. Larger single crystals of $[K(THF)][Mg(C_3H_5)_3]$ were obtained in lower yield when toluene was used as a precipitant instead of pentane.

^{1}H NMR (400.1 MHz, THF-d_8): δ = 1.75-1.80 (m, 2H, β-THF), 2.26 (d, $^3J_{HH}$ = 11.5 Hz, 12H, CH_2CHCH_2), 3.60-3.64 (m, 2H, α-THF), 6.35 (quint, $^3J_{HH}$ = 11.5 Hz, 3H, CH_2CHCH_2) ppm. A spectrum with identical chemical shifts, but integrals with relative intensity of four for the THF signals, was obtained for the compound prepared by method B. ^{13}C NMR (100.6 MHz, THF-d_8): δ = 26.54 (s, β-THF), 56.44 (s, CH_2CHCH_2), 68.40 (s, α-THF), 151.74 (s, CH_2CHCH_2) ppm. Anal. calcd. for $C_{13}H_{23}KMgO$ (258.72 g/mol): Mg, 9.39; found: Mg, 9.34 (a sample prepared by method B was analyzed).

$[K_2Mg(C_3H_5)_4(THF)_2]$ ($[8\cdot(THF)_2]$). A concentrated solution of $[K_2Mg(C_3H_5)_4]$ in THF/pentane (1:1; 1 mL) was cooled to –30 °C. After 7 d, a block-like, colorless single crystal had formed.

$[CaMg(C_3H_5)_4]$ (9). THF (1.0 mL) was added to a mixture of **1** (20 mg; 0.19 mmol) and **7** (23 mg; 0.19 mmol). All volatiles were removed from the yellow solution under reduced pressure. The residue was washed with pentane (2 × 3 mL) to give a pale yellow solid, which was dried in vacuo. The product contained substoichiometric amounts of THF (typically 0.21-0.25 equiv.). Yield: 37 mg, 0.15 mmol, 79%.

^{1}H NMR (400.1 MHz, THF-d_8): δ = 1.76-1.79 (m, 0.9H, β-THF), 2.32 (d, $^3J_{HH}$ = 11.8 Hz, 16H, CH_2CHCH_2), 3.60-3.64 (m, 0.9H, α-THF), 6.27 (quint, $^3J_{HH}$ = 11.8 Hz, 4H, CH_2CHCH_2,) ppm. ^{13}C NMR (100.6 MHz, THF-d_8, 298.2 K): δ = 26.54 (s, β-THF), 57.68 (s, CH_2CHCH_2), 68.40 (s, α-THF), 148.18 (s, CH_2CHCH_2) ppm. A sample containing 0.25 equiv. of THF according to ^{1}H NMR spectroscopy was used for microanalysis: Anal. calcd. for $(C_{12}H_{20}CaMg)\cdot(C_4H_8O)_{0.25}$ (246.70 g/mol): Ca, 16.25; Mg, 9.85; found: Ca, 16.49; Mg, 9.05.

Butadiene Polymerization. Butadiene/THF solutions (BD content: 5.05-7.81% (m/m)) were prepared by condensing the desired amount of monomer first over molecular sieve (4 Å) and then into a defined amount of dry THF. The butadiene content was determined gravimetrically. Polymerization experiments were typically run on a 50 μmol scale with respect to the initiator. In a typical experiment carried out at elevated temperature, a solution of the initiator in THF (0.5 mL) was added to the monomer solution and the reaction mixture was placed in a preheated oil bath. In a typical experiment carried out at lowered temperature, a septum sealed Schlenk flask containing the monomer solution was cooled to the desired temperature while stirring. After few minutes, a solution of the initiator in THF (0.5 mL) was injected. Reactions were terminated by addition of isopropanol (1.0 mL). After removal of a small aliquot for ^{1}H NMR spectroscopic determination of conversion, the reaction mixture was poured into a stirred solution of MeOH/HCl(conc.) (100 mL, 100:1). All volatiles were removed from the mixture and the resulting colorless polymer was dried in vacuo for 1 h at 70 °C. Gravimetrically and spectroscopically determined yields were in good agreement.

Reactions with Ethylene. In a typical NMR scale experiment, a solution of **5**/**6**/**8**/**9** (45 μmol) in THF-d_8 (0.5 mL) was degassed and pressurized with ethylene (2.0 bar). The course of the reaction was followed by NMR spectroscopy. In a typical lab scale experiment, a solution of **5**/**8** (0.60 mmol) in THF (1.0 mL) was degassed and pressurized with ethylene (2.0 bar). At

the end of the desired reaction time, excess ethylene was boiled off and the reaction was quenched with water (50 μL). The reaction mixture was filtered and analyzed by GC/MS.

[K(CH$_2$CH$_2$CH$_2$CH=CH$_2$)] (5-ins). ^{1}H NMR (400.1 MHz, THF-d_8): δ = 0.89 (t, 2H, $^3J_{HH}$ = 7.4 Hz, KC*H*$_2$CH$_2$CH$_2$CH=CH$_2$), 1.35-1.44 (m, 2H, KCH$_2$C*H*$_2$CH$_2$CH=CH$_2$), 2.01 (dt, 2H, $^3J_{HH}$ = 6.8 Hz, $^3J_{HH}$ = 7.5 Hz, KCH$_2$CH$_2$*CH*$_2$CH=CH$_2$), 4.90 (ddt, 1H, $^2J_{HH}$ = 2.3 Hz, $^3J_{HH}$ = 10.3 Hz, $^4J_{HH}$ = 1.0 Hz, KCH$_2$CH$_2$CH$_2$CH=C*H*^{cis}H^{trans}), 4.96 (ddt, 1H, $^2J_{HH}$ = 2.3 Hz, $^3J_{HH}$ = 17.1 Hz, $^4J_{HH}$ = 1.5 Hz, KCH$_2$CH$_2$CH$_2$CH=CH^{cis}*H*^{trans}), 5.78 (ddt, 1H, $^3J_{HH}$ = 6.8 Hz, 10.3 Hz, 17.1 Hz, KCH$_2$CH$_2$CH$_2$C*H*=CH$_2$) ppm. Resonances due to ethylene, unreacted **5**, and trace amounts of propene[53] were also detected.

[KMg(CH$_2$CH$_2$CH$_2$CH=CH$_2$)] (6-ins). ^{1}H NMR (400.1 MHz, THF-d_8): δ = –0.73 (t, 2H, $^3J_{HH}$ = 8.0 Hz, [Mg]C*H*$_2$CH$_2$CH$_2$CH=CH$_2$), 1.62 (tt, 2H, $^3J_{HH}$ = 7.8 Hz, $^3J_{HH}$ = 8.0 Hz, [Mg]CH$_2$C*H*$_2$CH$_2$CH=CH$_2$), 1.96 (dt, 2H, $^3J_{HH}$ = 7.0 Hz, $^3J_{HH}$ = 7.8 Hz, [Mg]CH$_2$CH$_2$*CH*$_2$CH=CH$_2$), 4.67 (ddt, 1H, $^2J_{HH}$ = 2.9 Hz, $^3J_{HH}$ = 10.0 Hz, $^4J_{HH}$ = 1.3 Hz, [Mg]CH$_2$CH$_2$CH$_2$CH=C*H*^{cis}H^{trans}), 4.80 (ddt, 1H, $^2J_{HH}$ = 2.9 Hz, $^3J_{HH}$ = 17.1 Hz, $^4J_{HH}$ = 1.5 Hz, [Mg]CH$_2$CH$_2$CH$_2$CH=CH^{cis}*H*^{trans}), 5.85 (ddt, 1H, $^3J_{HH}$ = 7.0 Hz, 10.0 Hz, 17.1 Hz, [Mg]CH$_2$CH$_2$CH$_2$C*H*=CH$_2$) ppm. ^{13}C NMR (100.6 MHz, THF-d_8): δ = 10.38 (br s, [Mg]*C*H$_2$CH$_2$CH$_2$CH=CH$_2$), 32.67 (s, [Mg]CH$_2$*C*H$_2$CH$_2$CH=CH$_2$), 45.13 (s, [Mg]CH$_2$CH$_2$*C*H$_2$CH=CH$_2$), 111.61 (s, [Mg]CH$_2$CH$_2$CH$_2$CH=*C*H$_2$), 143.51 (s, [Mg]CH$_2$CH$_2$CH$_2$*C*H=CH$_2$) ppm. Resonances due to ethylene, unreacted **6**, and trace amounts of propene[53] were also detected.

[K$_2$Mg(CH$_2$CH$_2$CH$_2$CH=CH$_2$)] (8-ins). ^{1}H NMR (400.1 MHz, THF-d_8): δ = –0.76 (t, 2H, $^3J_{HH}$ = 8.0 Hz, [Mg]C*H*$_2$CH$_2$CH$_2$CH=CH$_2$), 1.62 (tt, 2H, $^3J_{HH}$ = 7.8 Hz, $^3J_{HH}$ = 8.0 Hz, [Mg]CH$_2$C*H*$_2$CH$_2$CH=CH$_2$), 1.96 (dt, 2H, $^3J_{HH}$ = 6.8 Hz, $^3J_{HH}$ = 7.8 Hz, [Mg]CH$_2$CH$_2$*CH*$_2$CH=CH$_2$), 4.66 (ddt, 1H, $^2J_{HH}$ = 2.9 Hz, $^3J_{HH}$ = 10.0 Hz, $^4J_{HH}$ = 1.3 Hz, [Mg]CH$_2$CH$_2$CH$_2$CH=C*H*^{cis}H^{trans}), 4.80 (dd, 1H, $^2J_{HH}$ = 2.9 Hz, $^3J_{HH}$ = 17.2 Hz, $^4J_{HH}$ = 1.5 Hz,

[Mg]$CH_2CH_2CH_2CH{=}CH^{cis}H^{trans}$), 5.86 (ddt, 1H, $^3J_{HH}$ = 6.8 Hz; 10.0 Hz; 17.2 Hz, [Mg]$CH_2CH_2CH_2CH{=}CH_2$) ppm. ^{13}C NMR (100.6 MHz, THF-d_8): δ = 11.30 (br s, [Mg]$CH_2CH_2CH_2CH{=}CH_2$), 32.87 (s, [Mg]$CH_2CH_2CH_2CH{=}CH_2$), 45.27 (s, [Mg]$CH_2CH_2CH_2CH{=}CH_2$), 111.43 (s, [Mg]$CH_2CH_2CH_2CH{=}CH_2$), 143.73 ([Mg]$CH_2CH_2CH_2CH{=}CH_2$) ppm. Resonances due to ethylene, unreacted **8**, and trace amounts of propene[53] were also detected.

Computational Details. All calculations were performed with the Amsterdam Density Functional program (ADF2012.1).[54] For geometry optimization, the BP86-D3 functional was used; it is based on the local density approximation (LDA, Slater exchange and VWN correlation)[55] with gradient corrections[56] from Becke (exchange) and Perdew (correlation) added self-consistently. It also incorporates dispersion corrections according to Grimme's DFT-D3 method.[57] The TZ2P basis set was used for all calculations; it is an uncontracted set of Slater-type orbitals of triple-ζ quality, augmented by two sets of polarization functions (d and f on heavy atoms; 2p and 3d sets on H). For geometry optimization, core electrons (e.g., 1s for second and third periods, 1s2s2p for fourth-period (K) were treated by the small frozen core approximation.[58] For bond order analysis, the Nalewajski-Mrozek (N-M) bond indices, which incorporate both covalent and ionic contributions to bonding,[26] were used with equivalent all-electron basis sets. For **10c** and **10d**, frequency calculations were used with the same all-electron basis sets to establish the nature of stationary points and for thermodynamic results.

X-Ray Crystal Structure Determinations. Data were collected on a Bruker CCD area-detector diffractometer with Mo Kα radiation (graphite monochromator, λ = 0.71073 Å) using φ and ω scans. The SMART program package was used for the data collection and unit cell determination; processing of the raw frame data was performed using SAINT; absorption corrections were applied with SADABS.[59] The structures were solved by direct methods and

refined against F^2 using all reflections with the SHELXL-97 software. The non-hydrogen atoms were refined anisotropically, and hydrogen atoms were placed in calculated positions.[60]

Supplementary Material

Additional details of the polymerization reaction of **6**, **8**, and **9** with butadiene; the reaction of **5**, **6**, and **8** with ethylene; and the reaction of **6**, **8**, and **9** with pyridine. CIF files giving X-ray crystallographic data for **2**, **4**, **6**, and [**8**·$(THF)_2$]. Coordinates of the geometry optimized structures of **10a-d** and of the base-free complex [$(CH_3)_2Mg(THF)(C_3H_5)K$]. These are available free of charge via the Internet at http://pubs.acs.org.

Acknowledgements

The authors thank Lara Lemmerz for valuable contributions to experimental work, Dr. Elise Abinet for help in the single crystal X-ray structure determination of compound **2**, and Dr. Klaus Beckerle and Dr. Phillip Jochmann for helpful discussions. Financial support by Fonds der Chemischen Industrie (Kekulé scholarship to C. L.) is gratefully acknowledged. T. P. H. thanks the National Science Foundation (CHE-1112181) for support.

Graphic Material for Table of Contents

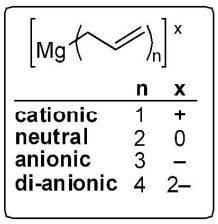

Unprecedented M–Allyl Bonding

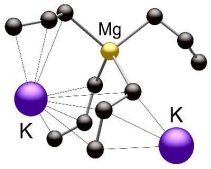

Polymerization Oligomerization

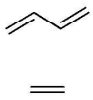

References

(1) (a) Richey, H. *Grignard Reagents: New Developments*; Wiley VCH: Chichester, 2000. (b) Benkeser, R. A. *Synthesis* **1971**, 347-358.

(2) (a) Marsch, M.; Harms, K.; Massa, W.; Boche, G.; *Angew. Chem.* **1987**, *99*, 706-707; *Angew. Chem. Int. Ed.* **1987**, *26*, 696-697. (b) Benn, R.; Lehmkuhl, H.; Mehler, K.; Rufińska, A. *Angew. Chem.* **1984**, *96*, 521-522; *Angew. Chem. Int. Ed.* **1984**, *23*, 534-535. (c) Hill, E. A.; Boyd, W. A.; Desai, H.; Darki, A.; Bivens, L.; *J. Organomet. Chem.* **1996**, *514*, 1-11. (d) Benn, R.; Lehmkuhl, H.; Mehler, K.; Rufińska, A. *J. Organomet. Chem.* **1985**, *293*, 1-6. (e) Solomon, S. A.; Muryn, C. A.; Layfield, R. A. *Chem. Commun.* **2008**, 3142-3144. (f) Chmely, S. C.; Carlson, C. N.; Hanusa, T. P.; Rheingold, A. L. *J. Am. Chem. Soc.* **2009**, *131*, 6344-6345. (g) Bailey, P. J.; Liddle, S. T.; Morrison, C. A.; Parsons, S. *Angew. Chem.* **2001**, *113*, 4595-4598; *Angew. Chem. Int. Ed.* **2001**, *40*, 4463-4466. (h) Vestergren, M.; Eriksson, J.; Håkansson, M. *J. Organomet. Chem.* **2003**, *681*, 215-224.

(3) (a) Noyori, R.; Suga, S.; Kawai, K.; Okada, S.; Kitamura, M. *Pure Appl. Chem.* **1988**, *60*, 1597-1606. (b) Sośnicki, J. G. *Tetrahedron Lett.* **2005**, *46*, 4295-4298. (c) Sośnicki, J. G. *Synlett* **2009**, *15*, 2508-2512. (d) Sośnicki, J. G.; Struk, L. *Synlett* **2009**, *11*, 1812-1816. (e) Sośnicki, J. G. *Tetrahedron Lett.* **2006**, *47*, 6809-6812. (f) Lipshutz, B. H.; Hackmann, C. *J. Org. Chem.* **1994**, *59*, 7437-7444. (g) Alvaro, G.; Boga, C.; Savoia, D.; Umani-Ronchi, A. *J. Chem. Soc., Perkin Trans. 1*, **1996**, 875-882. (h) Cainelli, G.; Giacomini, D.; Panunzio, M.; Zarantonello, P. *Tetrahedron Lett.* **1992**, *33*, 7783-7786. (i) Overly, K. R.; Williams, J. M.; McGarvey, G. J.; *Tetrahedron Lett.* **1990**, *31*, 4573-4576. (j) Yamamoto, Y.; Komnatsu, T.; Maruyama, K. *J. Chem. Soc., Chem. Commun.*

1985, 814-816. (k) Bogdanović, B.; Huckett, S. C.; Wilczok, U.; Rufińska, A. *Angew. Chem.* **1988**, *100*, 1569-1572; *Angew. Chem. Int. Ed.* **1988**, *27*, 1513-1516.

(4) (a) Li, F.; Jin, Y.; Pei, F.; Wang, F. *J. Macromol. Sci. A* **1994**, *A31*, 273-282. (b) Wu, W.; Chen, M.; Zhou, P. *Organometallics* **1991**, *10*, 98-104. (c) Ajellal, N.; Furlan, L.; Thomas, C. M.; Casagrande Jr, O. L.; Carpentier, J.-F. *Macromol. Rapid Commun.* **2006**, *27*, 338-343. (d) Sánchez-Barba, L. F.; Hughes, D. L.; Humphrey, S. M.; Bochmann, M. *Organometallics* **2006**, *25*, 1012-1020. (e) Sánchez-Barba, L. F.; Hughes, D. L.; Humphrey, S. M.; Bochmann, M. *Organometallics* **2005**, *24*, 5329-5334. (f) Jin, Y.; Li, F.; Pei, F.; Wang, F.; Sun, Y. *Macromolecules* **1994**, *27*, 4397-4398. (g) Ajellal, N.; Guillevic, E.; Thomas, C. M.; Jackstell, R.; Beller, M.; Carpentier, J.-F. *Adv. Synth. Catal.* **2008**, *350*, 431-438. (h) Yuan, M.; Xiong, C.; Li, X.; Deng, X. *J. Appl. Polym. Sci.* **1999**, *73*, 2857-2862. (i) Standfuss, S.; Abinet, E.; Spaniol, T. P.; Okuda, J. *Chem. Commun.* **2011**, *47*, 11441-11443.

(5) In this context, the term carbometalation describes the addition of a fragment M–R (M = metal, R = anionic organic ligand) across a multiple bond of an organic substrate.

(6) **3** carbometalates pyridine with >95% selectivity to give an *N*-metalated 1,2-dihydropyridine. However, the product is unstable and could not be isolated (for details see Supporting Information).

(7) The ^{1}H NMR spectrum of bis(allyl)magnesium in THF-d_8 shows an AX_4 pattern for the allyl ligands in the temperature range of –120 °C to 37 °C indicating fluxional behavior of the allyl ligand: Zieger, H. E.; Roberts, J. D. *J. Org. Chem.* **1969**, *34*, 1976-1977.

(8) A similar coordination geometry has been reported for [MgMe(14N4)][C_5H_5] (14N4 = 1,4,8,11-tetramethyl-1,4,8,11-tetraazacyclotetradecane): Pajerski, A. D.; Squiller, E. P.; Parvez, M.; Whittle, R. R.; Richey Jr., H. G. *Organometallics* **2005**, *24*, 809-814.

(9) Jaenschke, A.; Paap, J.; Behrens, U. *Z. Anorg. Allg. Chem.* **2008**, *634*, 461-469.

(10) *N*-Metalated dihydropyridines were obtained. Resonances indicative of a mixture of the 1,2- and the 1,4-carbometalation product were initially observed. The 1,2-product was slowly transformed into the 1,4-product. For details see Supporting Information.

(11) Coordination of THF to Mg rather than to the alkali ion has recently been reported for magnesiate [$LiMg(CH_2SiMe_3)_3(THF)$]: Baillie, S. E.; Clegg, W.; García-Álvarez, P.; Hevia, E.; Kennedy, A. R.; Klett, J.; Russo, L. *Organometallics* **2012**, *31*, 5131-5142.

(12) The K–C distances corresponding to the weak secondary K–C interactions exceed the value assumed for $K–C^{olefin}$ bonding, but are 14-15% below the sum of the van der Waals radii. Without these weak secondary interactions, there would be a bisphenoidal coordination geometry around K1, which is extremely unusual for potassium compounds.

(13) The weak secondary K–(η^1-C_3H_5) interactions were omitted in these considerations.

(14) (a) Strohmann, C.; Lehman, H.; Dilsky, S. *J. Am. Chem. Soc.*, **2006**, *128*, 8102-8103. (b) Engerer, L. K.; Carlson, C. N.; Hanusa, T. P.; Brennessel, W. W.; Young Jr., B. G. *Organometallics* **2012**, *31*, 6131-6138.

(15) [K(18-c-6)][$Al(C_3H_5)_4$] (a) and [K(18-c-6)][$Zn(C_3H_5)_3$] (b) have also been reported to show bridging coordination modes of the allyl ligand, but the exact bonding mode could not unambiguously be identified due to low diffraction intensities at high diffraction angles in single crystal X-ray analysis: (a) Lichtenberg, C.; Spaniol, T. P.; Okuda, J. *Organometallics* **2011**, *30*, 4409-4417. (b) See citation in ref. 20.

(16) Layfield, R. A.; Bullock, T. H.; García, F.; Humphrey, S. M.; Schüler, P. *Chem. Commun.* **2006**, 2039-2041.

(17) (a) Gren, C. K.; Hanusa, T. P.; Rheingold, A. L. *Main Group Chem.* **2009**, *8*, 225-235. (b) Quisenberry, K. T.; Gren, C. K.; White, R. E.; Hanusa, T. P.; Brennessel, W. W. *Organometallics* **2007**, *26*, 4354-4356. (c) Simpson, C. K.; White, R. E.; Carlson, C. N.; Wrobleski, D. A.; Kuehl, C. J.; Croce, T. A.; Steele, I. M.; Scott, B. L.; Young, Jr., V.

G.; Hanusa, T. P.; Sattelberger, A. P.; John, K. D. *Organometallics* **2005**, *24*, 3685-3691.

(18) Torvisco, A.; Decker, K.; Uhlig, F.; Ruhlandt-Senge, K.; *Inorg. Chem.* **2009**, *48*, 11459-11465 and references therein.

(19) Pronounced libration of at least one C atom in each allyl ligand prohibited the exact determination of the geometric parameters within the allyl ligands.

(20) Preliminary results on the synthesis and characterization of **8** have recently been reported: Lichtenberg, C.; Spaniol, T. P.; Perrin, L.; Maron, L.; Okuda, J. *Chem. Eur. J.* **2012**, *18*, 6448-6452.

(21) Lichtenberg, C.; Jochmann, P.; Spaniol, T. P.; Okuda, J. *Angew. Chem.* **2011**, *123*, 5872-5875; *Angew. Chem. Int. Ed.* **2011**, *50*, 5753-5756.

(22) Only few allyl compounds have been reported to form three dimensional networks in the solid state due to bridging allyl ligands, e. g.: (a) $[Zn(C_3H_5)_2]$ (ref. 25). (b) $[Cu_5Cl_5(C_3H_5)_4Si]$: Dużak, T.; Kinzhybalo, V.; Ślepokura, K.; Olijnyk, V. *Z. Anorg. Allg. Chem.* **2009**, *635*, 2324-2327.

(23) (a) Quisenberry, K. T.; White, R. E.; Hanusa, T. P.; Brennessel, W. W. *New J. Chem.* **2010**, *34*, 1579-1584. (b) See also citation in ref. 11.

(24) (a) Baillie, S. E.; Clegg, W.; Garcıá-Alvarez, P.; Hevia, E.; Kennedy, A. R.; Klett, J.; Russo, L. *Chem. Commun.* **2011**, *47*, 388-390. (b) Jochmann, P.; Davin, J. P.; Maslek, S.; Spaniol, T. P.; Sarazin, Y.; Carpentier, J.-F.; Okuda, J. *Dalton Trans.* **2012**, *41*, 9176-9181.

(25) Lichtenberg, C.; Engel, J.; Spaniol, T. P.; Englert, U.; Raabe, G.; Okuda, J. *J. Am. Chem. Soc.* **2012**, *134*, 9805-9811.

(26) (a) Michalak, A.; DeKock, R. L.; Ziegler, T. *J. Phys. Chem. A* **2008,** *112*, 7256-7263. (b) Nalewajski, R. F.; Mrozek, J., *Int. J. Quantum Chem.* **1994**, *51*, 187-200. (c)

Nalewajski, R. F.; Mrozek, J.; Michalak, A., *Int. J. Quantum Chem.* **1997**, *61*, 589-601. (d) Nalewajski, R. F.; Mrozek, J.; Mazur, G., *Can. J. Chem.* **1996**, *74*, 1121-1130.

(27) The K–C distance of 3.554 Å is close to the cut off value of 3.57 Å suggested for K–olefin bonds in the solid state (see ref. 18).

(28) Hsieh, H. L.; Wang, I. W. *Macromolecules*, **1986**, *19*, 299-304.

(29) $[Ca(C_3H_5)(18\text{-c-}6)][Zn(C_3H_5)_3]$ containing an allyl calcium monocation has also been reported not to initiate the polymerization of butadiene in THF solution (ref. 21).

(30) As previously reported for organoalkaline metal initiators, higher 1,2-PBD contents were obtained with initiators **6** and **8** at lower temperatures (see Supp. Inf.).

(31) Determined at –25 °C rather than at 0 °C to create a greater time frame for data collection.

(32) Such equilibria have been experimentally observed for $[Li_2CuMe_3]$ and $[Li_2ZnMe_4]$: (a) Mobley, T. A.; Müller, F.; Berger, S. *J. Am. Chem. Soc.* **1998**, *120*, 1333-1334. (b) Mobley, T. A.; Berger, S. *Angew. Chem.* **1999**, *111*, 3256-3258; *Angew. Chem. Int. Ed.* **1999**, *38*, 3070-3072.

(33) A similar trend has been observed for methyl methacrylate polymerization initiated by potassium allyl lanthanoid compounds: see ref. 17c.

(34) $[Ni(\eta^3\text{-}C_3H_5)\{P(OPh)_3\}_3][PF_6]$ was used as a catalyst at 25 °C in benzene: (a) Taube, R.; Gehrke, J.-P. *J. Organomet. Chem.* **1985**, *291*, 101-115. (b) Taube, R.; Schmidt, U.; Gehrke, J.-P.; Bohme, P.; Langlotz, J.; Wache, S. *Makromol. Chem. Makromol. Symp.* **1993**, *66*, 245-260.

(35) $[(\eta^5\text{-}C_5Me_5)_2Gd][B(C_6F_5)_4]$ / Al*i*Bu_3 was used a catalyst at low temperature (–78 to –40 °C) in toluene: (a) Kaita, S.; Yamanaka, M.; Horiuchi, A. C.; Wakatsuki, Y. *Macromolecules* **2006**, *39*, 1359-1363. (b) see citation in ref. 52a.

(36) Industrially used Ziegler Natta type catalysts based on ternary systems consisting of a transition metal (Ti, Co, Ni) or rare earth metal (Nd) salt, an organoaluminum

compound and a co-reagent such as water, iodine or [$BF_3(OEt_2)$] give PBD with *cis*-1,4-PBD contents of 93-98%: (a) Weissermel, K.; Arpe, H.-J. *Industrial Organic Chemistry*, 2nd Ed., Wiley-VCH: Weinheim, 1993, Chapter 17. (b) Porri, L.; Giamsso, A. *Conjugated Diene Polymerization*, in *Comprehensive Polymer Science*, Vol. 4, Part II (Eds.: Eastmond, G. C.; Ledwith, A.; Russo, S.; Sigwalt, B.), Pergamon, Oxford, 1989, pp. 53-108.

(37) *n*BuLi was used as an initiator in the presence of chelating bis(amino) ligands such as dimorpholinoethane at –5 to +20 °C: Halasa, A. F.; Lohr, D. F.; Hall, J. E. *J. Polym. Sci. Polym. Chem. Ed.* **1981**, *19*, 1357-1360.

(38) A quaternary catalyst system consisting of [$Co(acac)_3$] (acac = acetylacetonate)/ $AlEt_3$ / H_2O / CS_2 at 40 °C in benzene was used: Ashitaka, H.; Ishikawa, H.; Ueno, H.; Nagasaka, A. *J. Polym. Sci.* **1983**, *21*, 1853-1860.

(39) A combination of $AlEt_3$ and chromium complexes such as [$Cr(acac)_3$] (acac = acetylacetonate) or [$Cr(CO)_5(NC_5H_5)$] was used as a catalyst at 15 °C in benzene or toluene: (a) Natta, G.; Porri, L.; Zanini, G.; Palvarini, A. *Chim. Ind. (Milan)* **1959**, *41*, 1165-1169. (b) Bhowmick, A. K.; Stephens, H. L. *Handbook of Elastomers*, 2nd Ed., Marcel Dekker, New York, 2000.

(40) E. g.: Antkowiak, T. A.; Oberster, A. E.; Halasa, A. F.; Tate, D. P. *J. Polym. Sci. A* **1972**, *10*, 1319-1334.

(41) Lithium magnesiates generated in situ from *n*BuLi and [$Mg(n Bu)_2$] and used as initiators for BD polymerization in non-polar media gave 7-8% 1,2-PBD: see ref. 28.

(42) PBD with vinyl contents of ca. 70% have been investigated for industrial applications, e. g.: Yoshioka, A.; Komuro, K.; Ueda, A.; Watanabe, H.; Akita, S.; Masuda, T.; Nakajima, A. *Pure Appl. Chem.* **1986**, *58*, 1697-1706.

(43) Test reactions were carried out using the same monomer solutions as in case of entries 2-5 (Table 1); no protic impurities could be detected by ^{1}H NMR spectroscopy.

(44) (a) Jochmann, P.; Dols, T. S.; Spaniol, T. P.; Perrin, L.; Maron, L.; Okuda, J. *Angew. Chem.* **2010**, *122*, 7962-7965; *Angew. Chem. Int. Ed.* **2010**, *49*, 7795-7798. (b) Jochmann, P. *Diploma Thesis*, RWTH Aachen, 2008.

(45) Audureau, J.; Fointanille, M.; Sigwalt, P. *C. R. Acad. Sci.*, *Ser.C* **1972**, *275*, 1487-1490.

(46) Assadourian, L.; Gau, G. *Appl. Organomet. Chem.* **1991**, *5*, 167-172.

(47) (a) Podall, H. E.; Foster, W. E. *J. Org. Chem.* **1958**, *23*, 1848-1852. (b) Shepherd Jr., L. H. (Ethyl Corporation), US 3670038, **1970**. (c) Shepherd Jr., L. H. (Ethyl Corp.), US 3597487, **1971**.

(48) Farādy, L.; Bencze, L.; Markó, L. *J. Organomet. Chem.* **1969**, *17*, 107-116.

(49) Jochmann, P.; *Doctoral Thesis* 2011, RWTH Aachen.

(50) Possible reasons for differences between the reactivity of calcium and potassium compounds are given in the discussion of butadiene polymerization and also apply here.

(51) E. g.: Hoff, R.; Mathers, R. T. (Eds.), *Handbook of Transition Metal Polymerization Catalysts*, Wiley VCH, New Jersey, 2010 and references therein.

(52) (a) For 1,2- vs. 1,4-PBD: Kaita, S.; Hou, Z.; Nishiura, M.; Doi, Y.; Kurazumi, J.; Horiuchi, A. C.; Watasuki, Y. *Macromol. Rapid Commun.* **2003**, *24*, 179-184. (b) For *cis*-1,4- vs. *trans*-1,4-PBD: Frankland, J. A.; Edwards, H. G. M.; Hohnson, A. F.; Lewis, I. R.; Poshyachinda, S. *Spectrochim. Acta* **1991**, *47A*, 1511-1524 and references therein.

(53) Formation of propene was ascribed to reaction of the allyl compound with trace amounts of protic impurities in the ethylene, which could not be removed by passing the gas through a column of activated charcoal.

(54) ADF2012.01; SCM; Theoretical Chemistry; Vrije Universiteit; Amsterdam; The Netherlands; (http://www.scm.com).

(55) Vosko, S. H.; Wilk, L.; Nusair, M. *Can. J. Phys.* **1980**, *58*, 1200-1211.

(56) (a) Perdew, J. P.; *Phys. Rev. B* **1986**, *33*, 8822-8824. (b) Becke, A. D. *Phys. Rev. A* **1988**, *38*, 3098-3100.

(57) S. Grimme, J. Antony, S. Ehrlich, H. Krieg, *J. Chem. Phys.* **2010**, *132*, 154104/1-154104/19.

(58) Te Velde, G.; Bickelhaupt, F. M.; Baerends, E. J.; Fonseca Guerra, C.; Van Gisbergen, S. J. A.; Snijders, J. G.; Ziegler, T. *J. Comput. Chem.* **2001**, *22*, 931-967.

(59) Siemens ASTRO, SAINT and SADABS. Data Collection and Processing Software for the SMART System, Madison, WI, 1996.

(60) Sheldrick, G. M. *Acta Crystallogr. Sect. A* **2008**, *64*, 112-122.